

Refining light-use efficiency calculations for a deciduous forest canopy using simultaneous tower-based carbon flux and radiometric measurements

J.P. Jenkins^{a,*}, A.D. Richardson^a, B.H. Braswell^a, S.V. Ollinger^a,
D.Y. Hollinger^b, M.-L. Smith^b

^a University of New Hampshire, Complex Systems Research Center, Morse Hall, 39 College Road, Durham, NH 03824, USA

^b USDA Forest Service, Northern Research Station, 271 Mast Road, Durham, NH 03824, USA

Received 16 May 2006; received in revised form 8 November 2006; accepted 14 November 2006

Abstract

The concept of light-use efficiency (LUE) is the underlying basis for estimating carbon exchange in many ecosystem models, especially those models that utilize remote sensing to constrain estimates of canopy photosynthesis. An understanding of the factors that control the efficiency with which forest canopies harvest available light to fix carbon via photosynthesis is therefore necessary for the development of useful production efficiency models. We present an analysis of observations of daily LUE for 2004 in a northern hardwood stand at the Bartlett Experimental Forest CO₂ flux tower, White Mountains, New Hampshire (USA). We used eddy covariance measurements to estimate gross carbon exchange (GCE), and radiometric instruments mounted above and below the canopy to estimate the fraction of incident photosynthetically active radiation absorbed by the canopy (*f*APAR). Both GCE and *f*APAR show strong seasonal and day-to-day variability that contribute to temporal variation in LUE. During the middle of the growing season, when *f*APAR is relatively constant, day-to-day variation in LUE is largely explained ($r^2 = 0.85$) by changes in the ratio of diffuse to total downwelling radiation, but is not strongly correlated with any other measured meteorological variable.

We also calculated top-of-canopy NDVI based on measurements of reflected radiation at 400–700 and 305–2800 nm. Seasonal variation in this broadband NDVI paralleled that of the 500 m MODIS pixel containing the flux tower. The relationship between broadband NDVI and *f*APAR is approximately linear during green-up, but non-linear during autumn senescence. This seasonal hysteresis has implications for the use of remote sensing indices (such as NDVI or EVI) in satellite estimation of *f*APAR for production efficiency modeling.

© 2006 Elsevier B.V. All rights reserved.

Keywords: AmeriFlux; Bartlett Experimental Forest; Canopy optics; Eddy covariance; *f*APAR; LAI; Light-use efficiency; MODIS; NDVI; Phenology; Reflectance; Remote sensing

1. Introduction

One of the greatest sources of uncertainty in predictions of future climate scenarios can be attributed to a lack of knowledge about the terrestrial carbon cycle, particularly as related to the future levels of atmospheric CO₂ (IPCC Third Assessment; Houghton

* Corresponding author. Tel.: +1 603 862 4204;
fax: +1 603 862 0188.

E-mail address: julian.jenkins@unh.edu (J.P. Jenkins).

et al., 2001; Schimel et al., 2004). Our current knowledge of how CO₂ sources and sinks are distributed among and between the major landmasses in the northern hemisphere is relatively poor (Running et al., 1999). Understanding the controls on spatial and temporal patterns of surface–atmosphere CO₂ exchange is therefore needed so that improved predictions of future levels of atmospheric CO₂ can be made.

Many existing broad-scale models of ecosystem carbon exchange (e.g., MODIS GPP: Turner et al., 2003a; Zhao et al., 2005; CASA: Potter et al., 1993; GLO-PEM: Prince and Goward, 1995; VPM: Xiao et al., 2004) rely on estimates of photosynthetic light-use efficiency (LUE), that is, the amount of carbon fixed per unit of absorbed solar radiation:

$$P = \varepsilon \times fAPAR \times PAR = \varepsilon \times APAR \quad (1)$$

where P is carbon fixed through photosynthesis, ε the light-use efficiency and APAR is the absorbed photosynthetically active radiation (PAR).

These estimates are often derived from physiological models or vegetation-specific look-up tables. In a production efficiency modeling (PEM) framework (Ollinger et al., in press), the LUE concept is combined with remote sensing estimates of leaf area index (LAI) and/or the fraction of absorbed photosynthetic radiation ($fAPAR$) to predict primary productivity as a function of integrated daily or monthly downwelling solar radiation. Relationships used in these models are derived from Monteith's (1972) finding that productivity is a linear function of PAR intercepted by the canopy.

While remote sensing is the principal tool used to develop spatially extensive estimates of gross primary productivity (Running et al., 2004), detailed analyses of the performance of remote sensing based PEM algorithms are still needed (Turner et al., 2003b). For example, a persistent challenge for PEM algorithms in general has been the lack of understanding concerning factors controlling variation in LUE both within and among vegetation types; individual studies have suggested that LUE varies with factors such as stand age, species composition, soil fertility and foliar nutrients (Gower et al., 1999). Additionally, the relationship between the optical remote sensing based normalized difference vegetation index (NDVI) and $fAPAR$ is generally considered to be near-linear (Sellers, 1985; Ruimy et al., 1994; Paruelo et al., 1997; Los et al., 2000) and consequently NDVI is frequently used with an estimate of maximum LUE in PEM models to calculate productivity (Ruimy et al., 1999).

For a specific ecosystem, the light-use efficiency could be calculated by making observations of two key variables from Eq. (1): (1) rates of gross photosynthetic uptake (P_{gross}) by the system, and (2) the amount of incident PAR that is absorbed by the canopy (APAR; or, when expressed as a fraction of downwelling radiation, $fAPAR$). Networks of carbon flux towers (such as AmeriFlux and FLUXNET), where the surface–atmosphere exchange of CO₂ is being measured continuously in a wide range of ecosystems (Baldocchi et al., 2001), provide net ecosystem exchange, which can be used to estimate gross carbon exchange (GCE), a measure of P . Existing tower infrastructures also make it possible to conduct the necessary partitioning of the canopy radiation budget so that APAR can be determined. With these data, LUE, which has units of mol C per mol photon, could then be calculated as GCE/APAR.

In this paper, we present a comprehensive analysis of the factors affecting LUE in a northern hardwood forest in north-central New Hampshire, USA. We explore both annual and daily timescales as even PEMs which operate at this time step (Lagergren et al., 2005) generally assume constant annual LUEs. In addition, we investigate seasonal changes (i.e., phenology) in the optical properties of the canopy, as indicated by the temporal patterns of transmittance and reflectance. We use broadband radiation sensors to separately quantify changes in the reflectance of visible (VIS) and near-infrared (NIR) radiation.

2. Data and methods

2.1. Study site

The Bartlett Experimental Forest (44°17' N, 71°3' W) is located within the White Mountains National Forest in north-central New Hampshire, USA. The 1050 ha forest extends across an elevational range from 200 to 900 m a.s.l. It was established in 1931 and is managed by the USDA Forest Service Northeastern Research Station in Durham, NH. The climate is humid continental with short, cool summers (mean July temperature, 19 °C) and long, cold winters (mean January temperature, −9 °C). Annual precipitation averages 130 cm and is distributed evenly throughout the year. Soils are developed from glacial till and are predominantly shallow, well-drained spodosols. At low- to mid-elevation, vegetation is dominated by northern hardwoods (American beech, *Fagus grandifolia*; sugar maple, *Acer saccharum*; yellow birch, *Betula alleghaniensis*; with some red maple, *Acer rubrum* and paper birch, *Betula papyrifera*). Conifers (eastern hemlock,

Tsuga canadensis; eastern white pine, *Pinus strobus*; red spruce, *Picea rubens*) are occasionally found intermixed with the more abundant deciduous species but are generally confined to the highest (red spruce) and lowest (hemlock and pine) elevations. In 2003, the site was adopted as a NASA North American Carbon Program (NACP) Tier-2 field research and validation site. A more detailed description of the site is given elsewhere (Ollinger and Smith, 2005; <http://www.fs.fed.us/ne/durham/4155/bartlett.htm>).

A 26.5 m high tower was installed in a low-elevation northern hardwood stand in November, 2003, for the purpose of making eddy covariance measurements of the forest–atmosphere exchange of CO₂, H₂O and radiant energy. Continuous flux and meteorological measurements began in January, 2004, and are ongoing. Average canopy height in the vicinity of the tower is approximately 20–22 m. In the tower footprint, the forest is predominantly classified into red maple, sugar maple, and American beech forest types. Leaf area index in the vicinity of the tower is 3.6 as measured by seasonal litterfall collection, and 4.5 as measured by the optically based Li-Cor LAI-2000 instrument.

2.2. Radiometric measurements

Expressed formally, the forest canopy radiation budget is:

$$\text{APAR} = \text{PAR}_{\text{downwelling}} - \text{PAR}_{\text{reflected}} - \text{PAR}_{\text{transmitted}} + \text{PAR}_{\text{ground}} \quad (2)$$

where $\text{PAR}_{\text{downwelling}}$, $\text{PAR}_{\text{reflected}}$, and $\text{PAR}_{\text{transmitted}}$ are the incident, canopy reflected and canopy transmitted components of photosynthetically active radiation (400–700 nm) described below. $\text{PAR}_{\text{ground}}$ is visible radiation that is reflected by the forest floor. The fraction of absorbed PAR is given by

$$f\text{APAR} = \frac{\text{APAR}}{\text{PAR}_{\text{downwelling}}} \quad (3)$$

The tower is equipped with several broadband radiation sensors to measure photosynthetically active radiation (PAR) and global radiation (RAD). A pyranometer (model CM3, Kipp & Zonen B.V., Delft, The Netherlands; 305–2800 nm) and a quantum sensor (model 190SA, Li-Cor Inc., Lincoln, NE; 400–700 nm) are mounted on the tower at 25 m and face skyward to measure downwelling radiation ($\text{RAD}_{\text{downwelling}}$, $\text{PAR}_{\text{downwelling}}$). Another pyranometer and quantum sensor pair face down toward the top of the forest canopy and are mounted on a 3 m boom at 23.8 m and measure

upwelling radiation reflected by the canopy ($\text{RAD}_{\text{reflected}}$, $\text{PAR}_{\text{reflected}}$). A sunshine sensor (model BF3, Delta-T Devices Ltd., Cambridge, UK) is also mounted at 25 m, and is used to separate the direct beam and diffuse components of the incident photosynthetically active radiation ($\text{PAR}_{\text{direct}}$, $\text{PAR}_{\text{diffuse}}$). The sunshine sensor uses an array of photodiodes positioned under a perforated opaque dome, which is constructed in such a way that at least one photodiode is always in view of the sun (receiving $\text{PAR}_{\text{direct}} + 0.5 \times \text{PAR}_{\text{diffuse}}$), and at least one is in shadow (receiving $0.5 \times \text{PAR}_{\text{diffuse}}$). Diffuse, direct and total incident radiation is computed onboard using these sensor measurements. Further information about this sensor is available at <http://www.dynamax.com/bf2.htm>.

Below the canopy, an array of six quantum sensors, arranged in a circle of radius 15 m centered at the tower, are used to sample the heterogeneous below-canopy light environment ($\text{PAR}_{\text{transmitted}}$). The sensors (Li-Cor 190SA) are mounted on poles at a height of 1 m above the ground. We use the mean PPFD across all six sensors to estimate the flux of solar radiation transmitted through the canopy.

All instruments are connected to a data logger (model CR-10, Campbell Scientific Inc., Logan, UT). Measurements are recorded every 5 s and half-hourly summary data (mean, maximum, and standard deviation) are output to final storage. For this analysis, we only use data collected between 10 a.m. and 2 p.m. because this is when the sun is more directly overhead and canopy optics can differ at low sun angles. Additionally, this period is significant in terms of defining total daily carbon uptake and using all available half-hourly daytime measurements was not found to significantly impact the results described in this paper. Absorbed photosynthetically active radiation (APAR) was computed for each of the mean half-hourly samples during the mid-day period, corresponding with the available GCE data. These measurements were in turn averaged to produce a single mid-day average APAR and fractional APAR ($f\text{APAR}$). This time window and averaging methodology was used in the computation of all quantities (GCE, LUE, NDVI, etc.) in this study to ensure consistency.

We verified that in this optically dense (closed canopy) forest, light attenuation below the canopy was so great that observed visible radiation reflected from the forest floor was negligible during the growing season. Therefore, sensors to measure this final component of the canopy radiation budget were not installed and this flux ($\text{PAR}_{\text{ground}}$ in Eq. (2)) was not included in our radiation budget calculations.

Because NDVI is a reflectance index, radiances measured by the tower optical instruments must first be converted to total (r_{tot}) and visible spectrum (r_{vis}) reflectances using the ratio of upwelling to downwelling radiance.

$$r_{\text{tot}} = \frac{\text{RAD}_{\text{reflected}}}{\text{RAD}_{\text{downwelling}}} \quad (4a)$$

and

$$r_{\text{vis}} = \frac{\text{PAR}_{\text{reflected}}}{\text{PAR}_{\text{downwelling}}} \quad (4b)$$

and in terms of the observed quantities, the near-infrared reflectance was determined by assuming total measured reflectance is the average of visible and near IR (r_{vis}):

$$r_{\text{nir}} = 2 \times r_{\text{tot}} - r_{\text{vis}} \quad (5)$$

where r_{tot} , r_{nir} and r_{vis} are reflectance in the full, near IR and visible spectrums respectively. This assumption is justified through a comparison of MODIS mean visible and mean NIR through SWIR spectral channels in relation to total reflectance. We recognize that calculation of r_{nir} in this manner also includes reflectance in the shortwave infrared (as the pyranometer is sensitive to 2800 nm), whereas traditionally NDVI is calculated using approximately 700–1100 nm wavelengths in the NIR. For this reason we calculate NDVI from MODIS in two ways that are discussed below.

It is important to note that the quantum sensors measure photon flux density ($\mu\text{mol m}^{-2} \text{s}^{-1}$) while the pyranometers measure radiation in energy units (W m^{-2}). Nevertheless, our conversion of visible and total fluxes to dimensionless reflectances (Eqs. (4a) and (4b)) allows for a convenient solution to this problem and we were able to calculate NDVI as:

$$\text{NDVI}_{\text{tower}} = \frac{r_{\text{nir}} - r_{\text{vis}}}{r_{\text{nir}} + r_{\text{vis}}} \quad (6)$$

Although calculating total and visible reflectances first and assuming the total radiation is average of visible and NIR reflectance (Eq. (5)) conveniently negates the difference in measurement units between the sensors, we provide another verification of this approach. Huemmrich et al. (1999) give a conversion factor of $0.25 \text{ J } \mu\text{mol}^{-1}$ by which PAR measured by the quantum sensor can be expressed as W m^{-2} , the same units as the pyranometers. We recalculated r_{nir} directly as:

$$r_{\text{nir}} = \frac{\text{RAD}_{\text{reflected}} - (0.25 \times \text{PAR}_{\text{reflected}})}{\text{RAD}_{\text{downwelling}} - (0.25 \times \text{PAR}_{\text{downwelling}})} \quad (7)$$

Using this conversion factor, estimated NIR reflectance (Eq. (7)), and thus NDVI, was found to be almost exactly the same ($r^2 = 0.99$) as when calculated using Eqs. (4a), (4b) and (5). This, together with the MODIS test described above, validates the assumption made in Eq. (5) about relative weights of NIR and VIS within the total radiation spectrum.

During May and June of 2004 an automated dual channel spectrometer (model UniSpec-DC, PP Systems Inc., Amesbury, MA) was installed on the tower above the canopy. The spectrometer simultaneously measured visible and near IR downwelling and reflected radiation in 155 channels, evenly spaced from 400 to 900 nm, with bandwidths of 3.2 nm. The canopy-facing sensor was fixed at an angle of 45° down in a north-east direction from the tower, and approximately 10 noontime reflectance spectra per day were collected for each day the instrument was operational during the 2-month period of its installation.

2.3. Measurements and estimation of GCE

The forest-atmosphere CO_2 flux (NEE, or net ecosystem exchange) was measured at a height of 25 m with an eddy covariance system consisting of a model SAT-211/3K three-axis sonic anemometer (Applied Technologies Inc., Longmont, CO) and a model LI-6262 fast response $\text{CO}_2/\text{H}_2\text{O}$ infrared gas analyzer (Li-Cor Inc., Lincoln, NE), with data recorded at 5 Hz and fluxes (covariances) calculated every 30 min. The instrument configuration, calibration protocol, QA/QC, and data processing procedures were identical to those used at the Howland AmeriFlux site in central Maine, and are documented in more detail elsewhere (Hollinger et al., 2004).

For this study, we used a simple model to partition (Eq. (8a)) NEE to GCE and ecosystem respiration (R_{eco}). GCE is described by the commonly used, two-parameter, Michaelis–Menten light response function (Eq. (8b); e.g., Hollinger et al., 2004).

$$\text{NEE} = \text{GCE} + R_{\text{eco}} \quad (8a)$$

$$\text{GCE} = A_{\text{max}} \times \frac{\text{PAR}_{\text{downwelling}}}{K_m + \text{PAR}_{\text{downwelling}}} \quad (8b)$$

Here, A_{max} is the light-saturated rate of canopy photosynthesis, K_m is the half-saturation point of the light response function, and R_{eco} is treated as a constant, with model parameters fit to daytime flux measurements at the monthly time step. We used absolute deviations regression (Richardson and Hollinger, 2005), which yields maximum-likelihood parameter estimates given the

non-normal flux measurement error (Richardson et al., 2006). If NEE measurements were available, GCE was estimated as NEE minus the fitted parameter R_{eco} ; if there was a gap in the NEE record, then modeled GCE was estimated using Eq. (8b) with the best-fit A_{max} and K_{m} model parameters. Results were not appreciably different when nocturnal data were used to parameterize a more complex, temperature-dependent R_{eco} model. If fewer than six real half-hourly NEE observations were available (75% data coverage) during the 4 h mid-day window, the estimated GCE for this day was excluded from further analysis. However, during the growing season, less than 5% of days failed this criteria. Furthermore, based on a study at another site (Howland, ME), the statistical uncertainty of daily GCE values is not substantially greater on days with no observations (Hagen et al., 2006).

Average mid-daily GCE was calculated using the same 10 a.m. to 2 p.m. window as for the daily radiometric measurements. However, analysis of these data reveals a very strong linear correlation ($r^2 = 0.98$, $n = 366$) between the mid-day average GCE and total daily carbon uptake ($\text{GCE}_{\text{total}}$), and so we consider mid-day quantities to also be representative of daily averages (see also Sims et al., 2005). For convenience, here we define gross photosynthetic uptake (and hence LUE) to be a positive quantity.

2.4. MODIS data

For comparison with tower radiometric measurements, reflectance observations were obtained from the MODIS 16-day average Surface BRDF/Albedo product (MOD43). Data for the 500 m pixel that contains the tower footprint were extracted and the NIR (r_{nir}) and Red (r_{red}) reflectance channels used to calculate NDVI_{nir} :

$$\text{NDVI}_{\text{nir}} = \frac{r_{\text{nir}} - r_{\text{red}}}{r_{\text{nir}} + r_{\text{red}}} \quad (9)$$

An alternative method ($\text{NDVI}_{\text{nir+swir}}$), in which the average of all NIR and SWIR land channels was substituted for the r_{nir} term, was used to better replicate the spectral wavelengths included in the $\text{NDVI}_{\text{tower}}$ calculation (Eq. (6)).

We also used the blue reflectance channel (r_{blue}) to calculate the enhanced vegetation index (EVI) according to the standard MODIS production formula (Huete et al., 1999) and constants ($L = 1$, $C_1 = 6$, $C_2 = 7.5$ and $G = 2.5$):

$$\text{EVI} = G \times \frac{r_{\text{nir}} - r_{\text{red}}}{r_{\text{nir}} + C_1 \times r_{\text{red}} - C_2 \times r_{\text{blue}} + L} \quad (10)$$

MODIS estimates of 8-day average gross photosynthesis were obtained from the MOD17A2 composite product for the 1 km pixel containing the Bartlett tower for 2004. For the purpose of comparison to the flux estimated GCE used in this research the daily total MODIS data were scaled to mid-day averages using the strong linear relationship observed in the tower flux data and mentioned above.

With all MODIS products utilized in this research, variability of the 8 pixels surrounding the tower were analyzed with respect to the “center” pixel to avoid registration errors. Since the tower footprint is estimated to be less than 1 km, and the spatial variability across all 9 pixels was found to be insignificant, the pixel closest to the exact location of the tower was used. The overpass time for this satellite is about 10:30 a.m., which is within the mid-day window used for other calculations in this study.

2.5. Light-use efficiency calculation

The definition of LUE can vary as some studies use net productivity in the numerator and some gross photosynthesis (Schwalm et al., 2006). In this study, we define actual daily light-use efficiency (ϵ_0) of the canopy using the 4-h mid-day tower radiometric and CO_2 flux measurements as:

$$\epsilon_0 = \frac{\overline{\text{GCE}}}{\text{APAR}} \quad (11)$$

3. Results

3.1. Radiation budget

In this deciduous forest, there were strong seasonal patterns in the partitioning of the visible radiation budget, as indicated by data from 2004 (Fig. 1). The seasonality was largely driven by changes in canopy properties and associated changes in $f\text{APAR}$ (Fig. 2). In the winter (before DOY 100), a large fraction ($48 \pm 13\%$, mean ± 1 S.D.) of incident PAR reached the understory, and surface reflectance ($19 \pm 15\%$) was also high due to the presence of snow cover. In the middle of the growing season (DOY 160–280), only a very small fraction ($4 \pm 2\%$) of incident PAR reached the understory, and surface reflectance ($3 \pm 1\%$) was similarly low. In late autumn (after DOY 310), surface reflectance was similar to that in winter ($16 \pm 18\%$), but the fraction of radiation transmitted to the understory was lower ($35 \pm 14\%$) than in winter.

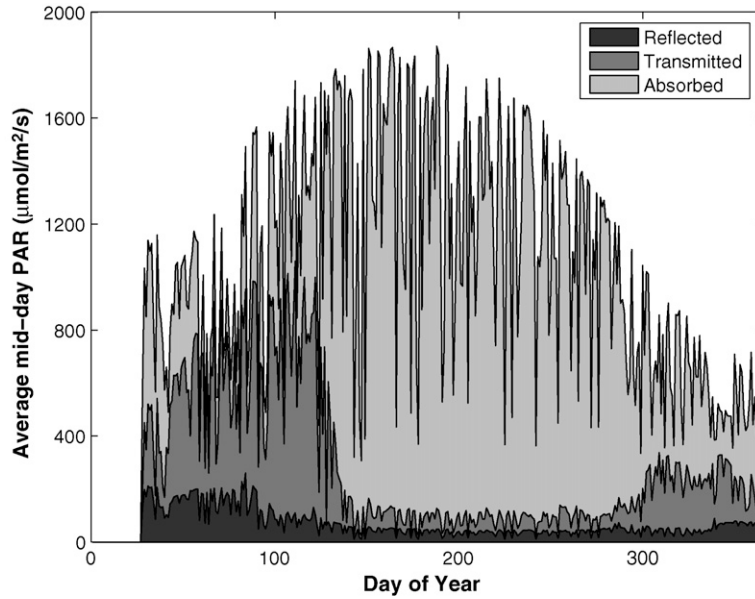


Fig. 1. Seasonal variation in the canopy radiation budget of a northern hardwood forest. Data are mid-day (10 a.m.–2 p.m.) averages. High transmitted values outside the growing season are due to the absence of leaves on the predominantly deciduous vegetation. Values of absorbed, transmitted and reflected PAR sum to incident PAR in the overlaid area plot.

The growing season itself could be divided into three relatively distinct periods (Fig. 2): (1) spring green-up, DOY 100–160, a period of rapid leaf growth and increasing optical density of the canopy, as

*f*APAR increased from the winter minimum (0.31 ± 0.16) to an essentially flat summertime plateau; (2) mid-growing season, DOY 160–280, when the canopy was fully developed and *f*APAR

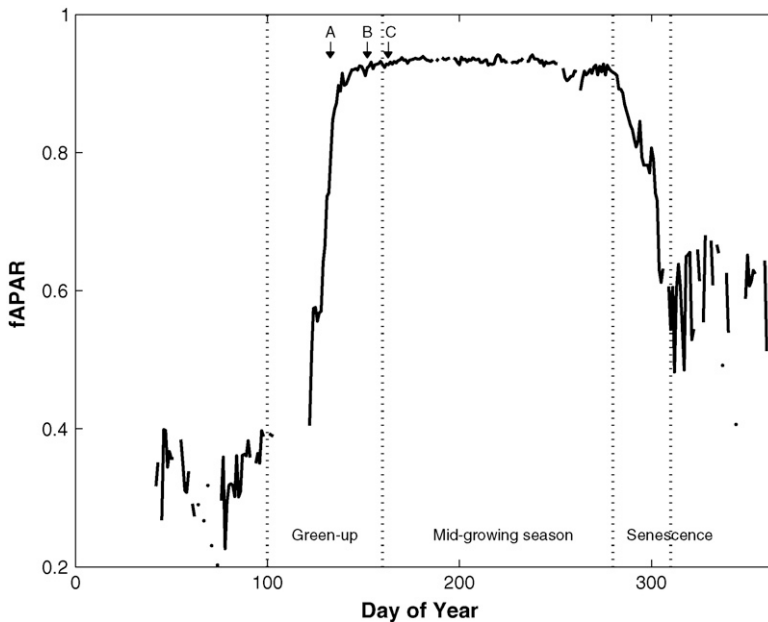


Fig. 2. Fraction of absorbed radiation (*f*APAR) for a forest canopy in 2004. Labeled dates correspond to days of high resolution spectrometry data (Fig. 10) where (A) May 12, (B) May 31, (C) June 11. Seasonal delineations were chosen through an analysis of these *f*APAR data and used to group data in the *f*APAR vs. NDVI relationship (Fig. 8).

varied little (0.93 ± 0.02); and (3) autumn senescence, DOY 280–310, when $fAPAR$ decreased relatively quickly from the summertime maximum as leaves were dropped and the canopy opened up again. By the end of this period of senescence, $fAPAR$ had declined to an intermediate value (0.48 ± 0.27) between the summer maximum and winter minimum.

3.2. Light-use efficiency and diffuse incident radiation

At Bartlett, average mid-day gross carbon exchange (GCE) (Fig. 3) showed a clearly defined seasonality due to seasonal climate variation and the deciduous nature of the canopy: GCE rose rapidly with spring onset and fell off sharply with autumn senescence. At Bartlett, GCE peaked around DOY 200 at a rate of $\approx 20 \mu\text{mol CO}_2 \text{ m}^{-2} \text{ s}^{-1}$, which is about 30% less than peak GCE at the deciduous Harvard Forest (Massachusetts) but about 20% higher than peak GCE at the spruce-dominated Howland Forest (Maine). The Bartlett ecosystem switched from being a CO_2 source to a CO_2 sink around DOY 130, and back to a CO_2 source around DOY 280 (results not shown). The carbon uptake period was much shorter at Bartlett than at the evergreen Howland Forest, where this period of positive CO_2 sequestration by the

vegetation extended from DOY 90–310. For illustrative purposes, MODIS estimated GCE is also included in Fig. 3. Mean MODIS gross carbon uptake during the 2004 growing season was 32% lower than mean tower estimates during this period for Bartlett. MODIS also predicted an approximately 3 weeks earlier onset of photosynthesis than we see in the tower data.

Over the course of the entire year phenological changes were the largest single control on both GCE (Fig. 3) and LUE (Fig. 4) as expected in a deciduous forest. During the growing season only, air temperature, soil temperature and vapor pressure deficit (VPD) were found to have significant but weak correlation with GCE ($r^2 \approx .2$, $P \leq 0.001$) and no significant correlation with LUE ($r^2 \approx 0$, $P > 0.15$) for mid-day averages at this site. One would expect VPD to exert a strong control on LUE due to limitations on stomatal conductance imposed at high VPD. Since VPD can vary at a high time frequency we examined the relationship between VPD and LUE using all mid-day half-hourly measurements. While the correlation between these two variables was found to be poor, a clear upper bound emerged from the relationship that describes the maximum possible LUE at a given VPD. As expected, maximum observed LUE decreased linearly with increasing

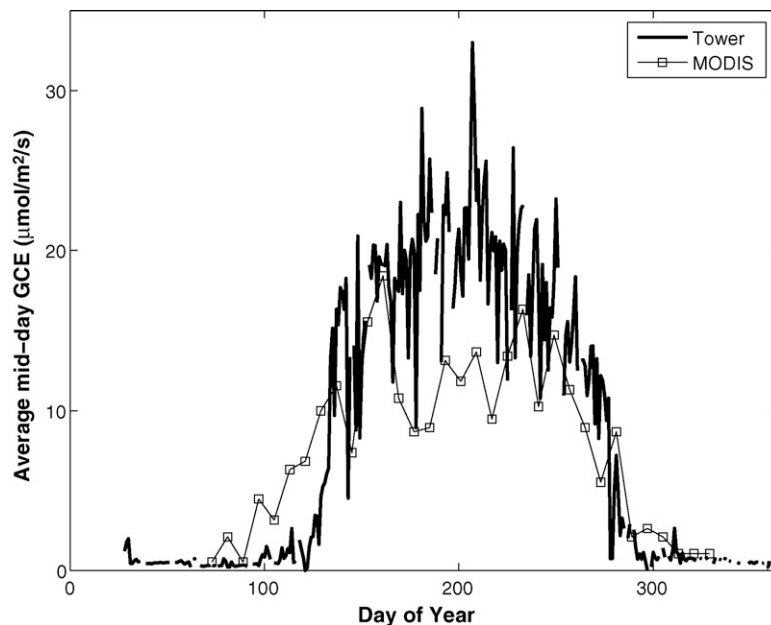


Fig. 3. Seasonal variation in daily mid-day mean gross carbon exchange (GCE) by a northern hardwood forest. GCE is calculated by adding estimated ecosystem respiration to the net ecosystem exchange of CO_2 measured by the eddy covariance system mounted on the tower. Data shown are mid-day average values (calculated from 10 a.m. to 2 p.m.). MODIS estimated gross photosynthesis from the 8-day composite product (MOD17) are considerably lower than tower estimates during the mid-growing season.

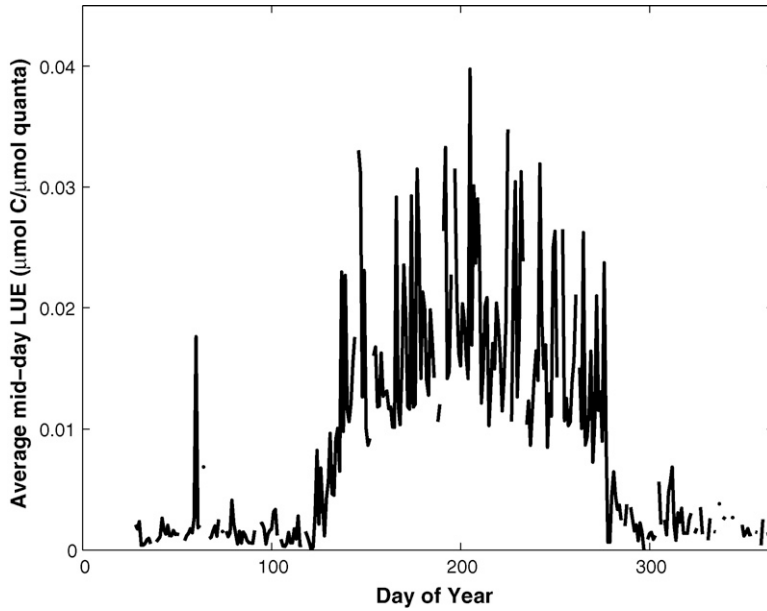


Fig. 4. Light-use efficiency (LUE) is calculated on a daily basis as average mid-day GCE/APAR. While APAR is relatively constant during the growing season, GCE is sensitive to environmental conditions and causes significant variability in LUE during these months.

VPD, however, VPD alone appears incapable of explaining the majority of high frequency variability in LUE below this bound. Of the environmental factors we examined, the only variable that proved to be a strong predictor of LUE (Fig. 5) during the peak

of the growing season was the diffuse:total PAR ratio, calculated with the above-canopy sunshine sensor ($r^2 = 0.85$, $P \leq 0.001$). As the diffuse:total ratio increased, the efficiency of the canopy in using the available light to drive carbon assimilation carbon

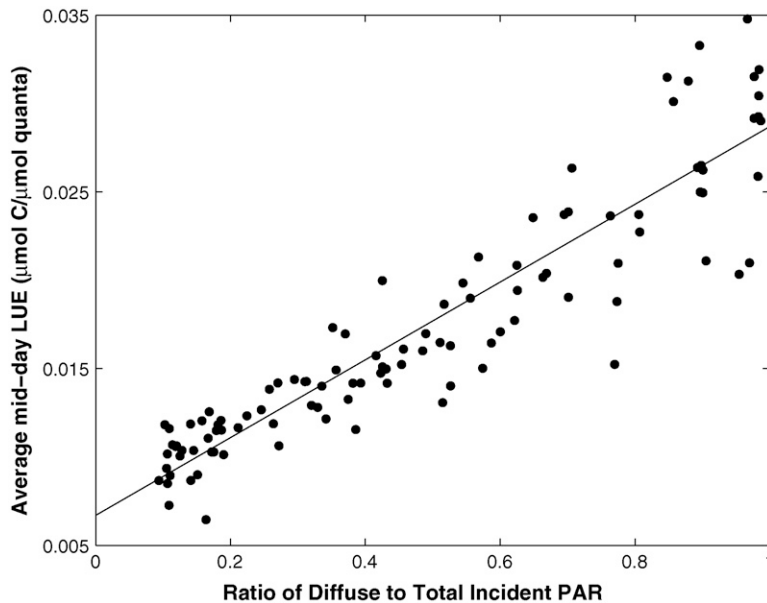


Fig. 5. Relationship between the diffuse fraction of incident PAR and light-use efficiency (LUE) of gross carbon uptake by forest canopy. Both quantities are averaged over a 4-h mid-day period. Data are filtered to show only the growing season (DOY 100–280), as this is when LUE has meaning. Under cloudy conditions (high % diffuse radiation), the incident PPFD is more efficiently used for photosynthesis than under sunny conditions (low % diffuse).

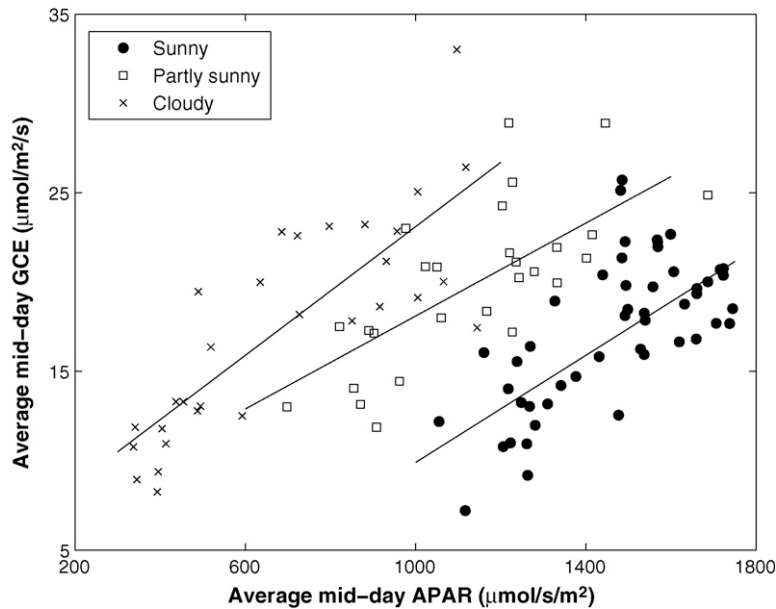


Fig. 6. Relationship of mid-day GCE to APAR under three cloudiness classifications: sunny (0–33% diffuse radiation), partly-sunny (33–66% diffuse) and cloudy (66–100% diffuse). For a given APAR, photosynthesis (GCE) is greater under increasingly cloudy conditions.

also increased. The observed LUE was roughly three-fold greater under completely overcast conditions (diffuse:total ratio ≈ 1) than under clear-sky conditions (diffuse:total ratio ≈ 0.1). Alternatively, Fig. 6

expresses this enhanced carbon uptake at a given level of absorbed radiation (i.e. LUE) by binning the diffuse:total radiation fraction into cloudy, partly sunny and sunny categories.

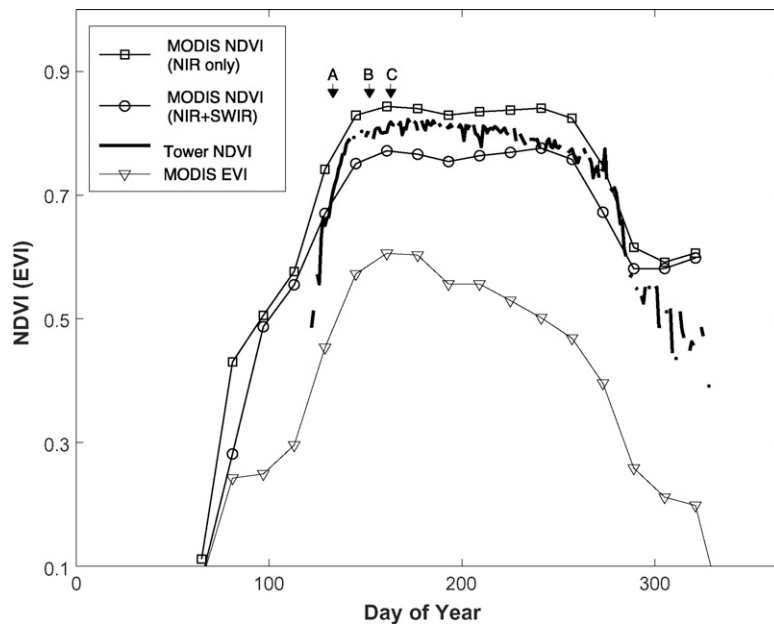


Fig. 7. Broadband normalized difference vegetation index (NDVI) calculated at the tower is compared to estimates of NDVI and EVI derived from the MOD43 surface reflectance product. Tower NDVI values are daily and MODIS are 16-day averages for the 500 m pixel containing the flux tower. Because the tower pyranometer is a broadband sensor with sensitivity beyond the NIR and into the SWIR, MODIS NDVI is calculated in two ways: (a) traditionally, using the NIR channel; and (b) using the combined NIR and SWIR reflectance in place of NIR alone. Note that the tower-measured NDVI generally falls between these two satellite values. MODIS EVI and tower NDVI both show a decrease across the growing season but MODIS NDVI does not. Labeled dates are the same as Fig. 2 and Fig. 10.

3.3. Seasonal patterns in spectral characteristics of canopy reflectance

Unlike NDVI calculated from MODIS products, $NDVI_{tower}$ was available continuously and was not subject to significant atmospheric interference. However, the 500 m MODIS pixel covered a far more spatially extensive area (including some patches of forest dominated by conifers) than the few trees (all deciduous) in the field of view of the tower-mounted instruments. In spite of these differences, seasonal changes in broadband $NDVI_{tower}$ were bracketed by the 16-day composite satellite-measured $NDVI_{nir}$ and $NDVI_{nir+swir}$ (Fig. 7). During the middle of the growing season, $NDVI_{nir}$ was about 10% higher, and $NDVI_{nir+swir}$ about 10% lower, than $NDVI_{tower}$. After a rapid rise in $NDVI_{tower}$ from DOY 120 to 150, $NDVI_{tower}$ reached a maximum value of around 0.81 at DOY 180 and then tapered off to a value of 0.75 at DOY 270. This gradual late-summer decline was not detected by either of the MODIS NDVI indices, which instead showed a mid-summer dip (and subsequent rebound) in NDVI around DOY 190. Both tower and satellite indices similarly captured the rapid drop in NDVI between DOY 270 and 290. In contrast to NDVI, MODIS calculated EVI (Fig. 7) does show a decline during the mid-growing season period like the tower data though

the degree of decline is more pronounced relative to the scale of the respective index.

At first glance, the seasonal patterns in $NDVI_{tower}$ (Fig. 7) appear similar to those in $fAPAR$ (Fig. 2); both showed strong responses that correspond to canopy development in the spring and senescence in the autumn. However, the relationship between $NDVI_{tower}$ and $fAPAR$ varied over the course of the growing season (Fig. 8). During the spring green-up, there was a strong linear correlation between the two quantities ($r^2 = 0.94$). However, because $NDVI_{tower}$ gradually declined after DOY 180, whereas $fAPAR$ was essentially constant until to DOY 280, this linear relationship became weaker by the middle of the growing season. $NDVI_{tower}$ was more sensitive to beginning stages of senescence than $fAPAR$, and from DOY 280 to 310, the relationship between $NDVI_{tower}$ and $fAPAR$ was non-linear and considerably offset from the linear relationship observed during green-up.

Canopy reflectance in the NIR evolved constantly over the entire growing season: it rose to a peak by DOY 150, and then gradually declined over the next 200 days (Fig. 9). On the other hand, over the course of spring green-up, VIS reflectance declined to a minimum at DOY 150. This minimum was maintained for roughly 100 days, before rising again between DOY 250 and

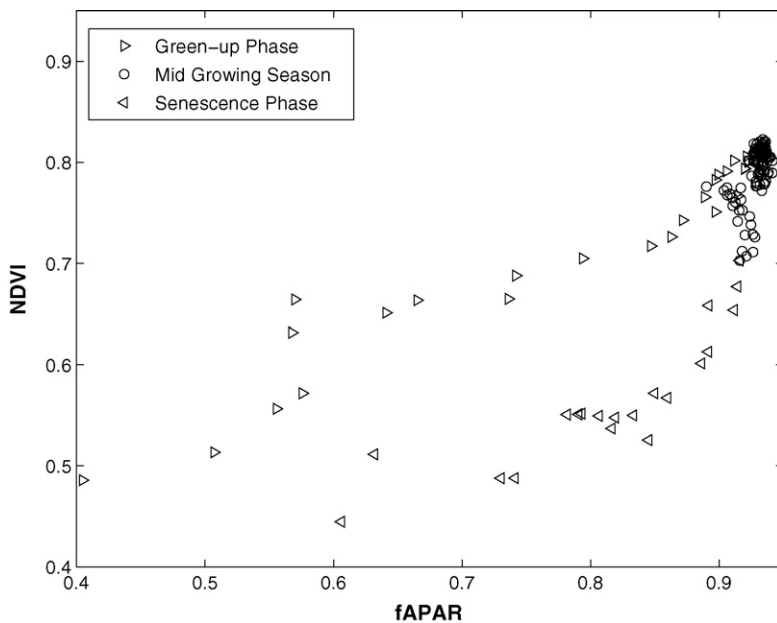


Fig. 8. Seasonal hysteresis in the relationship between broadband normalized difference vegetation index (NDVI) and the fraction of absorbed PAR ($fAPAR$). Data calculated from tower-mounted radiometric instruments, as described in text. Non-growing season data are not shown. Spring green-up (DOY 100–160), growing season (DOY 160–280) and autumn senescence (DOY 280–310) periods identified by inspection of $fAPAR$ time series (Fig. 2).

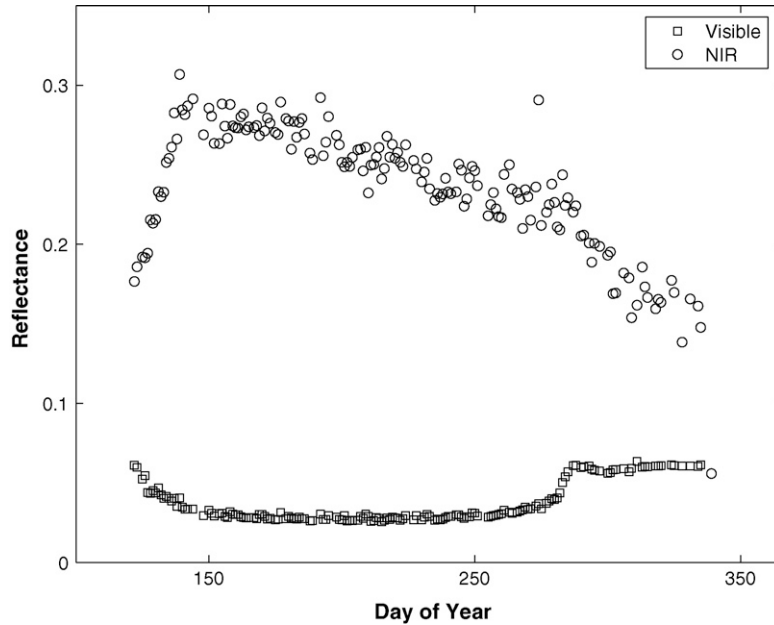


Fig. 9. Seasonal differences in visible and NIR spectrum reflectance at the Bartlett flux tower in 2004. NIR reflectance increases dramatically during leaf-out (~DOY 80–140) then decreases slowly throughout the growing season as the reflective properties of the chlorophyll pigments change. In contrast, visible reflectance is constant through the growing season until senescence. The relationship of reflectance in these two broadband spectral ranges is responsible for the seasonal f APAR–NDVI relationship observed in Fig. 8.

280. After DOY 280, VIS reflectance was constant, despite the ongoing decline in NIR reflectance (Fig. 9). The decrease in NIR reflectance relative to the constant VIS reflectance observed during the growing season

(DOY 150–280) was responsible for the decrease in NDVI during the same period (Fig. 7).

High spectral resolution reflectance data, collected during spring and early summer (DOY 130–190) by the

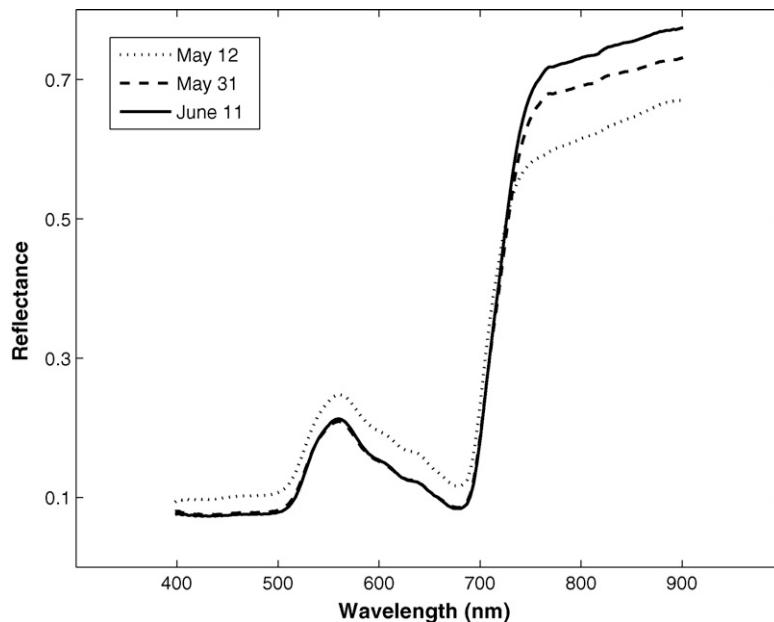


Fig. 10. Reflectance measured with a dual channel spectrometer mounted on the Bartlett flux tower during spring-early summer 2004. For the three dates shown, the depth of the red trough at 680 nm deepens and NIR reflectance increases as leaf structure develops and water content increases.

portable spectrometer mounted on the tower, provide further insight into temporal variation in the spectral distribution of canopy-reflected radiation (Fig. 10; the particular sampling dates selected are also illustrated on both Figs. 2 and 7). Changes in VIS reflectance can be associated with the development of foliar pigments (e.g., chlorophyll and carotenoids), whereas changes in NIR reflectance are associated with the anatomical or structural development, and possibly changes in leaf water content (Richardson et al., 2002; Richardson and Berlyn, 2002; Sims and Gamon, 2002). There was a more or less uniform decrease in reflectance across the entire visible range, but a somewhat larger increase in NIR reflectance above 725 nm, between DOY 133 and DOY 152. Between DOY 152 and DOY 163, there was little or no change in visible reflectance at any wavelength, but a continued increase in NIR reflectance above 700 nm. These results support the use of broadband observations at this site, in that no individual wavelengths (or groups of wavelengths) were found to be especially responsive to canopy development.

4. Discussion

While forest canopy LUE, in principle, can be influenced by a variety of environmental conditions and stresses, the results of this analysis indicates that the diffuse fraction of total incident radiation was the only significant control on daily variability of LUE at this site during the 2004 growing season. Phenological development was the principle control on both GCE and LUE over the course of the entire year as the study site was a deciduous forest. The effect of diffuse radiation either as a result of shade and cloudiness (Turner et al., 2003b; Gu et al., 1999; Healey et al., 1998; Hollinger et al., 1994) or aerosols (Gu et al., 2003; Roderick et al., 2001) on vegetation productivity can clearly be seen in our data. Global model inversions have tested the positive relationship between diffuse radiation and LUE at very broad scales (Still et al., 2004) using remote sensing together with an atmospheric transport model. A similar relationship between diffuse radiation and water use efficiency (WUE) has also been demonstrated (Min, 2005) using direct optical measurements. We used readily available radiometric field instruments to directly measure the diffuse:direct fraction coincident with flux measurements at a high temporal frequency and at a very focused spatial scale. The results show an even stronger linear relationship between the diffuse:total radiation fraction and LUE than previously documented (Rocha et al., 2004) and a larger effect than predicted by some

canopy radiative transfer models (Alton et al., 2005). Moreover, we show that the sensitivity of this trend extends across the full range of fractional diffuse radiation. These results support those presented in Schwalm et al. (2006) despite the fact that researchers in that study did not have the benefit of permanent below canopy and downward-facing above-canopy radiometric instruments to make direct measurements of light interception and absorption coincident with the flux measurements. The lack of covariance of LUE with air temperature and VPD indicate that, at this temporal resolution, the effect of diffuse radiation is optical or physiological in nature and not an indirect effect which leads to cooling air temperature over long time scales (Krakauer and Randerson, 2003; Robock, 2005). The theory behind the diffuse radiation and LUE relationship is conceptually straight forward: because leaf photosynthesis saturates at high light levels, allowing multiple leaves to be exposed to more moderate light levels will generally lead to higher canopy LUE than if the top leaf layers alone are exposed to intense direct beam radiation and the rest of the canopy is in deep shade (Roderick et al., 2001). Under cloudy or otherwise diffuse conditions, shadowing is considerably less and thus light is more evenly distributed between leaves throughout the canopy.

The relationship between LUE and diffuse:total ratio can also be partly explained by the fact that as the $PAR_{\text{downwelling}}$ is negatively correlated ($r^2 = -0.72$, $P < 0.001$) with the diffuse:total ratio. For example, when the diffuse:total ratio ≤ 0.33 , mean $PAR_{\text{downwelling}}$ is $\approx 1800 \mu\text{mol m}^{-2} \text{s}^{-1}$, which is more than twice the incident PAR as when the diffuse:total ratio > 0.66 . Thus, when the diffuse:total ratio is low, photosynthesis at the top of the canopy is light-saturated (lowest LUE) and the rest of the canopy is either poorly illuminated or also saturated in the case of sunflecks. When the diffuse:total ratio is high, canopy foliage as a whole operates in the steeper portions (higher LUE) of the hyperbolic light response function (Eq. (8b)) due to a more even distribution of light throughout the entire canopy. However, this only partially explains the correlation of LUE with the diffuse:total ratio because at a given APAR, GCE is highest (and hence LUE is higher) when the diffuse:total ratio > 0.66 , and lowest when the ratio ≤ 0.33 (Fig. 6). This reflects fundamental differences in the processing and utilization of diffuse versus direct beam radiation for photosynthesis by the canopy. Despite the fact that the diffuse fraction of incident solar irradiance is negatively correlated with fractional transmittance of solar irradiance through the atmosphere (Roderick et al., 2001) the relationship

between the diffuse:total ratio and LUE is stronger within our data than between incident PAR and LUE. Clouds and haze will simultaneously lead to both darker and more diffuse conditions but our results indicate that diffuse light reflects some aspect of LUE not captured by PAR alone. We believe this can be attributed light distribution within the canopy and does not simply indicate the top leaf layers are operating more efficiently at lower light levels. Both Hollinger (1996) and Urban et al. (in press) showed that transmitted light at various levels within a canopy represented a higher fraction of incoming PAR as the diffuse fraction of incident radiation increased, supporting the idea of a more uniformly illuminated canopy as the source of the enhancement. Gu et al. (2002) argues that incident radiation does not actually penetrate deeper into the canopy but rather describes this phenomenon as a redistribution of light from sunlit to shaded leaves under cloudy or turbid atmospheric conditions and that, since irradiance levels on leaves at all canopy depths and between leaves at all depths are more similar under diffuse conditions, the entire canopy may experience enhanced LUE.

Remote sensing derived production efficiency models generally incorporate vegetation-specific mean LUE parameters, though studies show that site variability can be most important in quantifying efficiency (Schwalm et al., 2006). Our results suggest that the inclusion of estimates of diffuse radiation (determined directly or through the inference of clouds and aerosols) as a scalar for LUE would substantially improve estimates of gross photosynthesis from such models, especially at daily time resolutions. Achieving this will require overcoming the challenge of estimating the diffuse radiation fraction over large areas in such a way that it can be integrated into existing production efficiency models. Diffuse conditions are often associated with sufficient cloud cover as to preclude the retrieval of optical parameters (Zhao et al., 2005), but this should not interfere with model based GCE estimates if $fAPAR$ is approximately constant during this period.

The relationship of $fAPAR$ and NDVI is also important to current remote sensing based efficiency models, as most use one or both of these indices to estimate APAR. Data presented in this paper (Fig. 8) indicate that the common assumption that $fAPAR$ scales as a linear function of NDVI is not tenable in this ecosystem. The main reason for this is that the canopy remained optically dense throughout the summer, and so $fAPAR$ varied little between the end of green-up and the beginning of senescence. By comparison, the spectral distribution of the canopy reflectance was

more sensitive to subtle changes in canopy properties (especially of topmost leaves), which were then captured by the spectral index, NDVI. Specifically, the change in NIR reflectance relative to VIS reflectance (Fig. 9) is responsible for the decrease in NDVI during the middle of the growing season. The decrease in NIR reflectance over the course of the growing season is likely the result of leaf aging. In tropical systems, an increase in leaf NIR absorbance (thus decreased reflectance) has been attributed to increased leaf necrosis and epiphytic growth as the leaf ages (Roberts et al., 1998). These factors lead to increased absorption in the NIR portion of the spectrum where scattering usually dominates. Similar findings were made in Eucalyptus vegetation (Stone et al., 2005). The impact of leaf aging on reflectance spectra and consequently NDVI is not usually accounted for in PEMs. The relationship between broadband NDVI and $fAPAR$ determined in this project stands in contrast to the results of Wang et al. (2004) who, in a similar study, found a linear relationship between these remote sensing indices for a pine forest in Finland. This discrepancy is likely related to the merging of temporal data in that study (3 years) and the different phenological patterns of deciduous and coniferous vegetation.

Correct assessment of annual total carbon uptake is often the objective of broad-scale PEMs but accomplishing this requires an accurate estimate of mean LUE. In a simple test, we were able to predict total annual carbon uptake at the tower using the mean LUE and $fAPAR$ (predicted through a linear relationship with tower calculated NDVI). This was the expected result (Ruimy et al., 1999), however this approach does not capture any of the daily variability in actual GCE and we had the advantage of knowing the actual mean LUE. Similarly, assuming a linear relationship between $fAPAR$ and NDVI may be adequate for annual productivity modeling, though some have suggested this leads to an over estimate of $fAPAR$ (Los et al., 2000). However, focused studies on phenologically important time periods (green-up and senescence phases) could be affected by the non-linear relationship between $fAPAR$ and remote sensing indexes explored in this paper. For example, chemical changes in leaves during senescence have been found to affect NDVI (Di Bella et al., 2004) through a change in reflectance properties before a reduction in displayed leaf area affects a change in $fAPAR$.

Despite the emergence of alternative vegetation indices such as EVI (Huete et al., 2002) and PRI (Guo and Trotter, 2004; Drolet et al., 2005), NDVI is still used

extensively in broad-scale mapping and ecosystem modeling activities. NDVI also has the longest record due to its ability to be calculated from AVHRR sensors. Even without atmospheric correction, our results showed a good agreement between MODIS NDVI and tower-based measurements of broadband NDVI for this forest.

5. Conclusions

Light-use efficiency is a critical parameter for many broad-scale carbon cycle models, yet the controls on LUE are poorly understood. Here we used a unique data set of coincident, tower-based radiometric instruments and flux-based GCE to explore the relative influence of a variety of environmental factors on LUE. Discounting the seasonal influence of phenological development, of all variables examined, the only one that explained a significant fraction of measured daily LUE was the ratio of diffuse to total incident solar radiation. Diffuse light generally arises as a result of atmospheric conditions (clouds, aerosols, etc.) which also lead to lower visible spectrum light levels at the surface and thus less photosynthetic saturation. In this study, the diffuse:total solar radiation ratio was found to have a stronger correlation with LUE than incident PAR. In addition to being associated with less saturating conditions at the top of the canopy, diffuse radiation causes less shadowing and allows a greater distribution of light from sunlit leaves to shaded leaves throughout the entire canopy. This increases overall LUE of the canopy by allowing light to reach otherwise shaded leaves and allowing leaves which might have been in direct sun to operate under less saturated conditions. Our results suggest that if existing production efficiency models are run at a monthly or higher frequency time step, consideration of the diffuse:total light ratio could make a substantial improvement in broad-scale carbon cycle modeling. Achieving this will require additional investment in methods for estimating diffuse radiation, using either remote sensing or predictive relationships based on other environmental variables that have yet to be identified. The non-linear relationship between f APAR and NDVI during the early and late portions of the growing season at this site also has implications for carbon cycle models that predict f APAR using satellite observed NDVI during these phenologically important time periods.

Acknowledgements

Bob Evans and Chris Costello are thanked for their assistance with tower operations. Support for this research was provided by the NASA Terrestrial Carbon

Program (Grant number: CARBON/04-0120-0011) and by the NASA IDS program (Grant number: NNG04GH75G). A.D.R. was supported by the Office of Science (BER), U.S. Department of Energy, through Interagency Agreement No. DE-AI02-00ER63028. Research at the Bartlett Experimental Forest is supported by the USDA Forest Service's Northern Global Change Program, and tower measurements are partially funded by USDA Forest Service Northeastern Research Station NACP. We thank PP Systems for the loan of the UniSpec DC spectrometer, and Andy Friedland, Dartmouth College, for the loan of data-loggers and meteorological sensors. Flux and meteorological data for the Bartlett tower are available at <http://public.ornl.gov/ameriflux/> subject to AmeriFlux "Fair-use" policies. This project is a contribution to the Hubbard Brook and Harvard Forest Long-Term Ecological Research Programs.

References

- Alton, P.B., North, P., Kaduk, J., Los, S., 2005. Radiative transfer modeling of direct and diffuse sunlight in a Siberian pine forest. *J. Geophys. Res.* 110:D23209 .
- Baldocchi, D., Falge, E., Gu, L., Olson, R., Hollinger, D., Running, S., Anthoni, P., Bernhofer, C., Davis, K., Evans, R., Fuentes, J., Goldstein, A., Katul, G., Law, B., Lee, X., Malhi, Y., Meyers, T., Munger, W., Oechel, W., Paw, U.K.T., Pilegaard, K., Schmid, H.P., Valentini, R., Verma, S., Vesala, T., Wilson, K., Wofsy, S., 2001. FLUXNET: a new tool to study the temporal and spatial variability of ecosystem-scale carbon dioxide, water vapor, and energy flux densities. *Bull. Am. Meteorol. Soc.* 82, 2415–2434.
- Di Bella, C.M., Paruelo, J.M., Becerra, J.E., Bacour, C., Baret, F., 2004. Effect of senescent leaves on NDVI-based estimates of f APAR: experimental and modelling evidences. *Int. J. Remote Sens.* 25 (23), 5415–5427.
- Drolet, G.G., Huemmrich, K.F., Hall, F.G., Middleton, E.M., Black, T.A., Barr, A.G., Margolis, H.A., 2005. A MODIS-derived photochemical reflectance index to detect inter-annual variations in the photosynthetic light-use efficiency of a boreal deciduous forest. *Remote Sens. Environ.* 98 (2/3), 212–224.
- Gower, S.T., Kucharik, C.J., Norman, J.M., 1999. Direct and indirect estimation of leaf area index, f (APAR), and net primary production of terrestrial ecosystems. *Remote Sens. Environ.* 70 (1), 29–51.
- Gu, L.H., Fuentes, J.D., Shugart, H.H., Staebler, R.M., Black, T.A., 1999. Responses of net ecosystem exchanges of carbon dioxide to changes in cloudiness: results from two North American deciduous forests. *J. Geophys. Res.* 104 (D24), 31421–31434.
- Gu, L.H., Baldocchi, D., Verma, S.B., Black, T.A., Vesala, T., Falge, E.M., Dowty, P.R., 2002. Advantages of diffuse radiation for terrestrial ecosystem productivity. *J. Geophys. Res.* 107:D5-64050 .
- Gu, L.H., Baldocchi, D.D., Wofsy, S.C., Munger, J.W., Michalsky, J.J., Urbanski, S.P., Boden, T.A., 2003. Response of a deciduous forest to the Mount Pinatubo eruption: enhanced photosynthesis. *Science* 299 (5615), 2035–2038.

- Guo, J.M., Trotter, C.M., 2004. Estimating photosynthetic light-use efficiency using the photochemical reflectance index: variations among species. *Funct. Plant Biol.* 31 (3), 255–265.
- Hagen, S.C., Braswell, B.H., Linder, E., Frolking, S., Richardson, A.D., Hollinger, D.Y., 2006. Statistical uncertainty of eddy flux-based estimates of gross ecosystem carbon exchange at Howland Forest, Maine. *J. Geophys. Res.* 111:D08S03 .
- Healey, K.D., Rickert, K.G., Hammer, G.L., Bange, M.P., 1998. Radiation use efficiency increases when the diffuse component of incident radiation is enhanced under shade. *Aust. J. Agric. Res.* 49 (4), 665–672.
- Hollinger, D.Y., Kelliher, F.M., Byers, J.N., Hunt, J.E., McSeveny, T.M., Weir, P.L., 1994. Carbon dioxide exchange between an undisturbed old-growth temperate forest and the atmosphere. *Ecology* 75, 134–150.
- Hollinger, D.Y., 1996. Optimality and nitrogen allocation in a tree canopy. *Tree Phys.* 16, 627–634.
- Hollinger, D.Y., Aber, J., Dail, B., Davidson, E.A., Goltz, S.M., Hughes, H., Leclerc, M.Y., Lee, J.T., Richardson, A.D., Rodrigues, C., Scott, N.A., Achuatavari, D., Walsh, J., 2004. Spatial and temporal variability in forest–atmosphere CO₂ exchange. *Glob. Change Biol.* 10, 1689–1706.
- Houghton, J.T., Ding, Y.D.J.G., Nogue, M., van der Linden, P.J., Xiaosu, D., 2001. Climate change 2001: the scientific basis. In: Contribution of Working Group I to the Third Assessment Report of the Intergovernmental Panel on Climate Change, Cambridge, UK, Cambridge University Press.
- Huemrich, K.F., Black, T.A., Jarvis, P.G., McCaughey, J.H., Hall, F.G., 1999. High temporal resolution NDVI phenology from micrometeorological radiation sensors. *J. Geophys. Res.* 104 (D22), 27935–27944.
- Huete, A., Justice, C., Team Members, 1999. MODIS Vegetation Index (MOD13) Algorithm Theoretical Basis Document, Version 3. Available from the GSFC Project Science Office.
- Huete, A., Didan, K., Miura, T., Rodriguez, E.P., Gao, X., Ferreira, L.G., 2002. Overview of the radiometric and biophysical performance of the MODIS vegetation indices. *Remote Sens. Environ.* 83 (1/2), 195–213.
- Krakauer, N.Y., Randerson, J.T., 2003. Do volcanic eruptions enhance or diminish net primary production? Evidence from tree rings. *Glob. Biogeochem. Cycles* 17:D041118 .
- Lagergren, F., Eklundh, L., Grelle, A., Lundblad, M., Molder, M., Lankreijer, H., Lindroth, A., 2005. Net primary production and light use efficiency in a mixed coniferous forest in Sweden. *Plant Cell Environ.* 28 (3), 412–423.
- Los, S.O., Collatz, G.J., Sellers, P.J., Malmstrom, C.M., Pollack, N.H., DeFries, R.S., Bounoua, L., Parris, M.T., Tucker, C.J., Dazlich, D.A., 2000. A global 9-yr biophysical land surface dataset from NOAA AVHRR data. *J. Hydrometeorol.* 1 (2), 183–199.
- Min, Q.L., 2005. Impacts of aerosols and clouds on forest–atmosphere carbon exchange. *J. Geophys. Res.* 110:D06203 .
- Monteith, J.L., 1972. Solar radiation and productivity in tropical ecosystems. *J. Appl. Ecol.* 9, 747–766.
- Ollinger, S.V., Treuhaft, R.N., Braswell, B.H., Anderson, J.E., Martin, M.E., Smith, M.L., in press. The role of remote sensing in the study of terrestrial net primary production. In: Fahey, T. (Ed.), *Methods for Estimating Net Primary Productivity. The Long-Term Ecological Research Network Series.* Oxford University Press.
- Ollinger, S.V., Smith, M.-L., 2005. Net primary production and canopy nitrogen in a temperate forest landscape: an analysis using imaging spectroscopy, modeling and field data. *Ecosystems* 8 (7), 760–778.
- Paruelo, J.M., Epstein, H.E., Lauenroth, W.K., Burke, I.C., 1997. ANPP estimates from NDVI for the Central Grassland Region of the United States. *Ecology* 78 (3), 953–958.
- Potter, C.S., Randerson, J.T., Field, C.B., Matson, P.A., Vitousek, P.M., Mooney, H.A., Klooster, S.A., 1993. Terrestrial ecosystem production—a process model-based on global satellite and surface data. *Glob. Biogeochem. Cycles* 7, 811–841.
- Prince, S.D., Goward, S.N., 1995. Global primary production: a remote sensing approach. *J. Biogeogr.* 22, 815–835.
- Richardson, A.D., Berlyn, G.P., 2002. Changes in foliar spectral reflectance and chlorophyll fluorescence of four temperate species following branch cutting. *Tree Physiol.* 22, 499–506.
- Richardson, A.D., Duigan, S.P., Berlyn, G.P., 2002. An evaluation of noninvasive methods to estimate foliar chlorophyll content. *New Phytologist* 153, 185–194.
- Richardson, A.D., Hollinger, D.Y., 2005. Statistical modeling of ecosystem respiration using eddy covariance data: maximum-likelihood parameter estimation, and Monte Carlo simulation of model and parameter uncertainty, applied to three simple models. *Agric. Forest Meteorol.* 131, 191–208.
- Richardson, A.D., Hollinger, D.Y., Burba, G.G., Davis, K.J., Flanagan, L.B., Katul, G.G., Munger, J.W., Ricciuto, D.M., Stoy, P.C., Suyker, A.E., Verma, S.B., Wofsy, S.C., 2006. A multi-site analysis of random error in tower-based measurements of carbon and energy fluxes. *Agric. Forest Meteorol.* 136, 1–18.
- Roberts, D.A., Nelson, B.W., Adams, J.B., Palmer, F., 1998. Spectral changes with leaf aging in Amazon caatinga. *Trees-Struct. Funct.* 12 (6), 315–325.
- Robock, A., 2005. Cooling following large volcanic eruptions corrected for the effect of diffuse radiation on tree rings. *Geophys. Res. Lett.* 32:L06702 .
- Rocha, A.V., Su, H.B., Vogel, C.S., Schmid, H.P., Curtis, P.S., 2004. Photosynthetic and water use efficiency responses to diffuse radiation by an aspen-dominated northern hardwood forest. *Forest Sci.* 50 (6), 793–801.
- Roderick, M.L., Farquhar, G.D., Berry, S.L., Noble, I.R., 2001. On the direct effect of clouds and atmospheric particles on the productivity and structure of vegetation. *Oecologia* 129, 21–30.
- Ruimy, A., Saugier, B., Dedieu, G., 1994. Methodology for the estimation of terrestrial net primary production from remotely sensed data. *J. Geophys. Res.* 99 (D3), 5263–5284.
- Ruimy, A., Kergoat, L., Bondeau, A., 1999. Participants potsdam NPP model intercomparison. Comparing global models of terrestrial net primary productivity (NPP): analysis of differences in light absorption and light-use efficiency. *Glob. Change Biol.* 5, 56–64.
- Running, S.W., Baldocchi, D.D., Turner, D.P., Gower, S.T., Bakwin, P.S., Hibbard, K.A., 1999. A global terrestrial monitoring network integrating tower fluxes, flask sampling, ecosystem modeling and EOS satellite data. *Remote Sens. Environ.* 70, 108–127.
- Running, S.W., Nemani, R.R., Heinsch, F.A., Zhao, M.S., Reeves, M., Hashimoto, H., 2004. A continuous satellite-derived measure of global terrestrial primary production. *Bioscience* 54 (6), 547–560.
- Sellers, P.J., 1985. Canopy reflectance, photosynthesis and transpiration. *Int. J. Remote Sens.* 6 (8), 1335–1372.
- Schimel, D.S., Churkina, G., Braswell, B.H., Trembath, J., 2004. Remembrance of weather past: ecosystem response to climate variability. In: Ehleringer, J. (Ed.), *A History of Atmospheric CO₂ and its Effects on Plants, Animals and Ecosystems.* Springer-Verlag, pp. 350–368.
- Schwalm, C.R., Black, T.A., Amiro, B.D., Arain, M.A., Barr, A.G., Bourque, C.P.-A., Dunn, A.L., Flanagan, L.B., Giasson, M.-A., Lafleur, P.M., Margolis, H.A., McCaughey, J.H., Orchansky, A.L.,

- Wofsy, S.C., 2006. Photosynthetic light use efficiency of three biomes across an east–west continental-scale transect in Canada. *Agric. Forest Meteorol.* 140 (1–4), 269–286.
- Sims, D.A., Gamon, J.A., 2002. Relationships between leaf pigment content and spectral reflectance across a wide range of species, leaf structures and developmental stages. *Remote Sens. Environ.* 81, 337–354.
- Sims, D.A., Rahman, A.F., Cordova, V.D., Baldocchi, D.D., Flanagan, L.B., Goldstein, A.H., Hollinger, D.Y., Misson, L., Monson, R.K., Schmid, H.P., Wofsy, S.C., Xu, L.K., 2005. Midday values of gross CO₂ flux and light use efficiency during satellite overpasses can be used to directly estimate eight-day mean flux. *Agric. Forest Meteorol.* 131, 1–12.
- Still, C.J., Randerson, J.T., Fung, I.Y., 2004. Large-scale plant light-use efficiency inferred from the seasonal cycle of atmospheric CO₂. *Glob. Change Biol.* 10 (8), 1240–1252.
- Stone, C., Chisholm, L., McDonald, S., 2005. Effects of leaf age and psyllid damage on the spectral reflectance properties of *Eucalyptus saligna* foliage. *Aust. J. Bot.* 53 (1), 45–54.
- Turner, D.P., Ritts, W.D., Cohen, W.B., Gower, S.T., Zhao, M.S., Running, S.W., Wofsy, S.C., Urbanski, S., Dunn, A.L., Munger, J.W., 2003a. Scaling Gross Primary Production (GPP) over boreal and deciduous forest landscapes in support of MODIS GPP product validation. *Remote Sens. Environ.* 88, 256–270.
- Turner, D.P., Urbanski, S., Bremer, D., Wofsy, S.C., Meyers, T., Gower, S.T., Gregory, M., 2003b. A cross-biome comparison of daily light use efficiency for gross primary production. *Glob. Change Biol.* 9, 383–395.
- Urban, O., Janous, D., Acosta, M., Czerny, R., Markova, I., Navratil, M., Pavelka, M., Pokorny, R., Sprtova, M., Zhang, R., Spunda, V., Grace, J., Marek, M.V., in press. Ecophysiological controls over the net ecosystem exchange of mountain spruce stand. Comparison of the response in direct versus diffuse solar radiation. *Glob. Change Biol.*
- Wang, Q., Tenhunen, J., Dinh, N.Q., Reichstein, M., Vesala, T., Keronen, P., 2004. Similarities in ground- and satellite-based NDVI time series and their relationship to physiological activity of a Scots pine forest in Finland. *Remote Sens. Environ.* 93, 225–237.
- Xiao, X.M., Zhang, Q.Y., Braswell, B.H., Urbanski, S., Boles, S., Wofsy, S., Berrien, M., Ojima, D., 2004. Modeling gross primary production of temperate deciduous broadleaf forest using satellite images and climate data. *Remote Sens. Environ.* 91 (2), 256–270.
- Zhao, M.S., Heinsch, F.A., Nemani, R.R., Running, S.W., 2005. Improvements of the MODIS terrestrial gross and net primary production global data set. *Remote Sens. Environ.* 95 (2), 164–176.